crystals

MDPI

Article

Characterization and Antibacterial Response of Silver Nanoparticles Biosynthesized Using an Ethanolic Extract of *Coccinia indica* Leaves

Suresh V. Chinni [1,*], Subash C. B. Gopinath [2], Periasamy Anbu [3], Neeraj Kumar Fuloria [4], Shivkanya Fuloria [4], Praveena Mariappan [1], Kishonthani Krusnamurthy [1], Lebaka Veeranjaneya Reddy [5], Gobinath Ramachawolran [1], Subramaniam Sreeramanan [6,7,8] and Sumitha Samuggam [1]

1 Department of Biotechnology, Faculty of Applied Sciences, AIMST University, Bedong 08100, Kedah, Malaysia; praveenadevi700@gmail.com (P.M.); kishon.0507@gmail.com (K.K.); gobinath_03@yahoo.com (G.R.) sumitha@aimst.edu.my (S.S.)
2 Institute of Nano Electronic Engineering and Faculty of Chemical Engineering Technology, Universiti Malaysia Perlis, Kangar 01000, Perlis, Malaysia; subash@unimap.edu.my
3 Department of Biological Engineering, Inha University, Incheon 402-751, Korea; anbu25@yahoo.com
4 Department of Pharmaceutical Chemistry, Faculty of Pharmacy, AIMST University, Bedong 08100, Kedah, Malaysia; neerajkumar@aimst.edu.my (N.K.F.); shivkanya_fuloria@aimst.edu.my (S.F.)
5 Department of Microbiology, Yogi Vemana University, Kadapa-516005, India; lvereddy@gmail.com
6 School of Biological Sciences, Universiti Sains Malaysia (USM), Minden Heights, Gelugor 11800, Penang, Malaysia; sreeramanan@usm.my
7 School of Bioprocess Engineering, Universiti Malaysia Perlis (UNIMAP), Arau 02600, Perlis, Malaysia
8 National Poison Centre, Universiti Sains Malaysia (USM), Gelugor 11800, Penang, Malaysia
* Correspondence: cvsureshgupta@gmail.com or v_suresh@aimst.edu.my; Tel.: +60-0124362324

Abstract: The present study was planned to characterize and analyze the antimicrobial activity of silver nanoparticles (AgNP) biosynthesized using a *Coccinia indica* leaf (CIL) ethanolic extract. The present study included the preparation of CIL ethanolic extract using the maceration process, which was further used for AgNP biosynthesis by silver nitrate reduction. Biosynthetic AgNPs were characterized using UV–Visible spectrometry, zeta potential analysis, transmission electron microscopy (TEM), scanning electron microscopy (SEM), atomic force microscopy (AFM), X-ray diffraction (XRD), and energy-dispersive X-ray (EDX) spectrometry. The biogenic AgNP and CIL extracts were further investigated against different bacterial strains for their antimicrobial activity. The surface plasmon resonance (SPR) signal at 425 nm confirmed AgNP formation. The SEM and TEM data revealed the spherical shape of biogenic AgNPs and size in the range of 8 to 48 nm. The EDX results verified the presence of Ag. The AgNPs displayed a zeta potential of −55.46 mV, suggesting mild AgNP stability. Compared to Gram-positive bacteria, the biogenic AgNPs demonstrated high antibacterial potential against Gram-negative bacteria. Based on the results, the current study concluded that AgNPs based on CIL extract have strong antibacterial potential, and it established that AgNP biosynthesis using CIL ethanol extract is an effective process.

Keywords: *Coccinia indica*; green synthesis; silver nanoparticle; characterization; antimicrobial

check for updates

Citation: Chinni, S.V.; Gopinath, S.C.B.; Anbu, P.; Fuloria, N.K.; Fuloria, S.; Mariappan, P.; Krusnamurthy, K.; Veeranjaneya Reddy, L.; Ramachawolran, G.; Sreeramanan, S.; et al. Characterization and Antibacterial Response of Silver Nanoparticles Biosynthesized Using an Ethanolic Extract of *Coccinia indica* Leaves. *Crystals* **2021**, *11*, 97. https://doi.org/10.3390/cryst11020097

Received: 27 December 2020
Accepted: 21 January 2021
Published: 22 January 2021

1. Introduction

Evidence shows that humans possess a 1:1 ratio of bacteria and human cells; minor disturbances of this ratio can result in multiple illnesses and diseases [1]. Widespread use of antibiotics results in multiple drug resistance (MDR) against infections and presents a high mortality risk [2]. To resolve the barriers associated with traditional antibiotic preparation, an extensive body of research on metallic nanoparticles has been documented over the past decade. Widespread application of silver nanoparticles (AgNPs) to improve antimicrobials

and other biological medicines, among the suggested metallic nanocomposites, has drawn much research attention [3].

AgNPs of 1–100 nm in size are more extensively used in nanoscience and technology. AgNPs offer high catalytic reactivity and antimicrobial activity [4,5]. AgNPs can be produced using various processes, such as chemical reduction, microwave irradiation, heat evaporation, and electrochemical reduction. However, the synthesis of AgNPs through these methods demands surface passivators (such as thiourea) to inhibit agglomeration, which may pollute the environment [6]. Another solution is to use a chemical process for AgNP synthesis. However, this may contribute to the adsorption of toxic elements over the particle surface and result in negative impacts. Hence, techniques that result in high yield while at the same time are environmentally-friendly, safe, and non-toxic are seriously being sought [7]. The merits associated with green synthesis, such as simplicity, stability, environmental friendliness, reproducibility, and cost-effectiveness, rationalize the importance of green AgNP synthesis [8]. Nanoparticle synthesis that involves plant material is considered an excellent green strategy [9]. Although AgNP synthesis using plant extracts as reductants does not produce harmful by-products, the organic compounds in leaf extracts impact the stability and reduction mechanisms of AgNPs [10–12].

Research suggests that, across the globe, antimicrobial resistance may cost around $1 trillion annually by the year 2050 [13]. The rising cost of medicines or antibiotics globally has stimulated investigators to conduct research and develop antibiotics using plant sources. Antimicrobials from plant sources offer high therapeutic efficacy, as they effectively treat various infectious diseases and mitigate common side effects associated with conventional antimicrobials [14]. The medicinal effects of plant products generally derive from combinations of various secondary metabolites found in the plants, such as tannins, alkaloids, steroids, flavonoids, phenolic compounds, fatty acids, steroids, resins, and gums [15]. *Coccinia indica (C. indica)*, the "perennial climber", has long drawn research attention due to its high antimicrobial potential. *C. indica* bearing tendrils is also known as ivy gourd. *C. indica* belongs to the Cucurbitaceae family and has been reported to be found in China, tropical Asia, Australia, Philippines, Indonesia, Thailand, Malaysia, and Myanmar. Various parts of the *C. indica plant* have been reported as having potential in the treatment of ringworm, smallpox, ulcers, itchy skin eruption, and psoriasis [16]. The phytochemicals present in *C. indica*, such as like saponins, cardenolides, flavonoids, and polyphenols possess high antibacterial potential [17]. In Ayurvedic medicine, *C. indica* is known for its hypoglycemic and antidiabetic properties. Evidence suggests that *C. indica* leaves (CIL) possess high antimicrobial, antioxidant, antidiabetic, hepato-protective, anti-inflammatory, chemo-protective, and antihyperlipidemic activities [18]. The concerns over the rising costs of antibiotics, as well as the associated benefits and antimicrobial potential of green AgNP and *C. indica* together were the motivation for the present investigation, which is to perform an antimicrobial evaluation of AgNPs biosynthesized from CIL extract. Hence, the present study was designed with a view to biosynthesizing cost-effective AgNPs with high antibacterial potential.

2. Materials and Methods

2.1. Plant Sample Collection

The leaves of *C. indica* were obtained from Semeling, Sungai Petani (Sungai Petani, Kedah, Malaysia) during the month of November, 2016. The leaves were washed, dried at room temperature in the shade, and reduced into small pieces. The chemicals, including silver nitrate ($AgNO_3$), Muller–Hinton agar, and dimethyl sulfoxide (DMSO) were procured from Fisher chemicals (Hampton, NH, USA), Hi-Media (Mumbai, Maharashtra, India), SD Fine (Mumbai, Maharashtra, India), and Sigma–Aldrich, (St. Louis, MI, USA). The glassware was cleaned and rinsed with deionized water and kept at 160 °C for 2 h. Plasticware was autoclaved before initiation of the antimicrobial experiment.

2.2. Extract Preparation

The CIL extract was prepared as per the standard procedure given in the systematic research literature with slight modification [19]. Briefly, 50 g of plant sample was transferred into 250 mL of 99.98% ethanol (1:5 ratio) in a volumetric flask. The conical flask was covered with aluminum foil and placed in an incubator shaker at 180 rpm at 37 °C for 1 week. Next, Whatman No. 1 filter paper was used to filter the plant extract. The extract was then condensed at low temperature (32–40 °C) by evaporation using a rotary evaporator. The concentrated extract was poured into a glass petri plate and left inside a fume chamber overnight for removal of the excess solvent. The petri plate was then sealed with parafilm, protected with foil, and placed in a refrigerator at 4 °C until further use.

2.3. Green Synthesis of AgNP

Then, 1 mM of silver nitrate solution was prepared by correctly dissolving 0.0085 g of silver nitrate in 45 mL of autoclaved distilled H_2O. A magnetic stirrer was used to stir the mixture for 10 min. To the stirred $AgNO_3$ solution, 5 mL of CIL extract was accurately applied drop by drop until the color changed from colorless to brownish green. The obtained mixture was incubated overnight at room temperature in completely dark conditions. Once the $AgNO_3$ solution was reduced (color changed to brown), it was then centrifuged at 10,000 rpm for 15 min to separate the AgNP. A few drops of distilled water were mixed with the resulting AgNP pellet. The pellet was scraped out, poured onto watch glass, and kept in air for complete drying. After complete drying, the dried particles were scraped out using a sterile scalpel blade and stored at room temperature [2].

2.4. UV–Visible Analysis of AgNP

The success of AgNP biosynthesis was verified using UV–Visible spectrometry. A small aliquot of AgNP was diluted in deionized water. The surface plasmon resonance (SPR) signal was detected by testing the reaction mixture with the UV–Visible spectrometer (Shimadzu UV–VIS-U2800 (Shimadzu, Kyoto, Kyoto, Japan)) at room temperature with a scanning speed of 300 nm/min. The measurements were made between 400 and 800 nm. The decrease in Ag^+ ions was determined by the UV–visible absorption spectrum of AgNP. At 430 nm, the AgNP solution exhibited an SPR peak.

2.5. Characterization of AgNP

As described in other research studies, pure AgNPs were used for characterization studies [20,21]. AgNP were routinely washed and centrifuged using deionized water prior to characterization with AgNP characterization data in order to prevent interaction of unbound residual biochemical entities of CIL extract. Different analytical techniques including zetasizer analysis, atomic force microscopy (AFM), energy-dispersive X-ray (EDX), X-ray diffraction (XRD), scanning electron microscopy (SEM), and transmission electron microscopy (TEM) were used to characterize AgNPs. The hydrodynamic diameter of AgNPs was analyzed by a Zeta-PAL zeta potential analyzer (Brookhaven Instruments, Holtsville, NY, USA). To determine the morphology of the AgNPs, TEM, and SEM measurements were carried out. The crystal nature of AgNPs was determined based on the analysis of their XRD spectrum recorded on a PANalytical X'Pert PRO MRD PW 3040/60 X-ray diffractometer (Malvern panalytical, Malvern, UK) using CuKα radiation (λ = 1.5406) at 40 kV to 40 mA in $2\theta/\theta$ scanning mode. The EDX spectrum was recorded using an FEI Nova NanoSEM 450 EDX unit (FEI, Hillsboro, OR, USA). AFM assisted in the determination of the presence and size distribution of biosynthesized AgNPs. For AFM analysis, dilute samples (0.05 mg/mL in water) of AgNP were spread over zinc substrate. Evaluation of sample topography (with 1×1 μm^2 scanned area) was performed at a set point of 10 nm with a scanning rate of 1 μm/s. The images were analyzed using a Bruker Dimension 3100 with Nanoscope 5 software (Bruker, Dynamostraße 19, Mannheim, Germany).

2.6. Antimicrobial Activity of AgNP

2.6.1. Disk Preparation

The plant extract (20 mg) and AgNPs (20 mg) were diluted separately in 1 mL of sterile 10% DMSO and mixed well. Next, the 50 µL of prepared plant extract and AgNP solution were separately added drop by drop on the top of 6 layered autoclaved Whatman® 70 mm Microfiber Filter Paper (Sigma-Aldrich, St. Louis, MI, USA), Grade CF/C disc, which was 6 mm in diameter. The disk was left to dry in a laminar hood at room temperature for 2 h. A ciprofloxacin disc and 10% DMSO were used as positive and negative controls, respectively.

2.6.2. Inoculum Preparation

To determine the antimicrobial potential of AgNP, 14 bacteria were used, namely *Escherichia coli* (*E. coli*), *Salmonella typhi* (*S. typhi*), *Proteus mirabilis* (*P. mirabilis*), *Enterobacter cloacae* (*E. cloacae*), *Vibrio cholera* (*V. cholera*), *Acinetobacter baumannii* (*A. baumannii*), *Staphylococcus aureus* (*S. aureus*), *Staphylococcus haemolyticus* (*S. haemolyticus*), *Staphylococcus epidermidis* (*S. epidermidis*), *Streptococcus pyogenes* (*S. pyogenes*), *Pseudomonas aeruginosa* (*P. aeruginosa*), *Klebsiella pneumoniae* (*K. pneumoniae*), *Lactobacillus*, and *Bacillus subtilis* (*B. subtilis*). These bacteria were streaked on nutrient agar from glycerol stock to obtain a single colony, and the plates were incubated overnight. A single colony from each bacterium was inoculated in nutrient broth (7 mL) and incubated for 5 h in an incubator shaker until it reached 0.6–0.7 OD at 600 nm absorbance level using a UV–Vis spectrometer. Next, each bacterial culture was diluted to achieve a viable cell count of 10^6 CFU/mL, standardized by 0.5 MacFarland.

2.6.3. Antibacterial Study

Antimicrobial evaluation of AgNP was based on disk diffusion methodology [22]. The strains of bacteria were swabbed over Mueller–Hinton agar (MHA) using sterile cotton swabs. Disks with ethanolic plant extract, AgNPs, 10% DMSO (negative control), and ciprofloxacin antibiotics (positive control) were applied over MHA agar. After 16 h of incubation, the zone of inhibition (ZOI) diameters (in mm) of each plates were measured.

3. Results and Discussion

3.1. Characterization of Synthesized Nanoparticles

The success of synthesis of AgNPs was based on results of visual inspection and UV–Visible spectrometric analysis. For color shift control, mixtures of $AgNO_3$ solution and CIL extract were held apart for 60 min at 60 °C. The change in color from yellow to brown after 60 min indicated the formation of AgNPs. The formation of AgNP in brown color solution was further confirmed by UV–Visible analysis, which generated an absorption spectrum comprising curves 1, 2, and 3 (Figure 1). Curve 1 represented the $AgNO_3$, curve 2 represented AgNP, and curve 3 represented CIL extract solution. The presence of an SPR peak at 425 in curve 2 of the UV–Visible spectrum confirmed formation of AgNPs. In the spectrum, curve 3 of the CIL extract did not exhibit a signal near 425 nm.

The AgNP formation was attributed to exposure of $AgNO_3$ to CIL extract, which reduced Ag^+ to Ag^0. The transition in color from yellow to brown as well as the UV–Visible signal at 425 nm were attributed to the property of surface plasmon resonance and stimulated by the possibility of plasmon vibrations [23].

The SEM and TEM derived size distribution histogram data assisted in the determination of the size and shape of AgNPs. The SEM data given in Figure 2A indicated that synthesized AgNP are spherical in shape and poly-dispersed. The average size distribution histogram based on TEM data (given in Figure 2(B1,B2,C), and Table 1) revealed AgNPs to exist in sizes ranging between 1 and 50 nm.

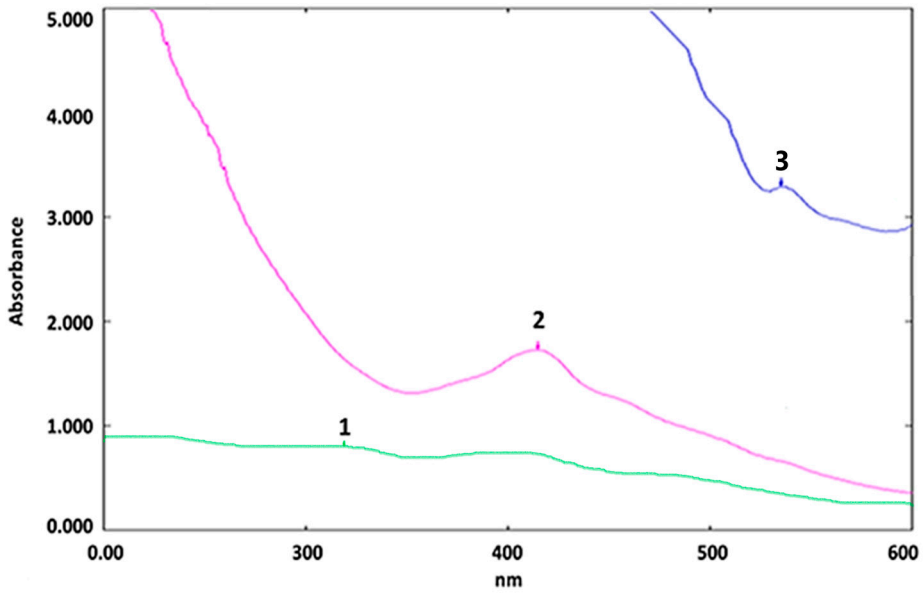

Figure 1. UV–Visible spectrum of silver nitrate solution (curve 1), AgNP (curve 2), and *Coccinia indica* leaf (CIL) extract (curve 3).

Scanning of AgNPs in tapping mode generated two-dimensional (2D) (Figure 3A and three-dimensional (3D) (Figure 3B images. The images confirmed the uniform distribution of AgNPs, as most of the particles sizes were consistent with the SEM and TEM measurements.

The EDX analysis by FESEM generated a spectrum, as seen in Figure 4. The spectrum revealed the elemental composition of AgNPs. EDX spectra determined silver (64.05%) as a major constituent element in comparison to chlorine (20.75%) and calcium (15.20%).

Prominent peak at 3 keV confirmed the presence of AgNP elemental silver. The presence of strong signals for silver and other elemental peaks may be attributed to biomolecules bounded to the surface of silver nanoparticles, indicating the reduction in silver ions to elemental silver.

For zeta potential analysis, the AgNP samples (50 µg/mL) were suspended in deionized water and measured in triplicate at 25 °C [24]. Zeta potential assists in determining the stability of AgNP. It is important to note that particles with zeta potential values more positive than +30 mV or more negative than −30 mV are considered to be stable [25]. In the present study the zeta potential of AgNP with −55.46 mV indicated and supported the stability of AgNP biosynthesized using CIL (Figure 5).

The XRD data specified in Figure 6 exhibited the crystalline nature of AgNP. The spectrum exhibited various diffraction signals at the angle of 2θ ranging from 10 to 90°. The four distinctive diffraction Braggs signals at 2θ values of 32°, 46°, 68°, and 78° could be indexed to the 113, 210, 220, and 311 reflection planes, respectively, of face-centered cubic structures of silver. Such a pattern confirmed the crystallinity of AgNPs. In addition to the Bragg peaks representative of AgNPs, some additional peaks were also observed. These peaks were attributed to biomolecules of CIL extract and were responsible for the reduction and stabilization of silver ions into the resultant silver nanoparticles [26,27].

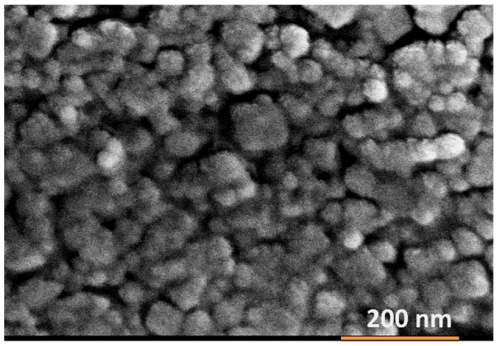

A

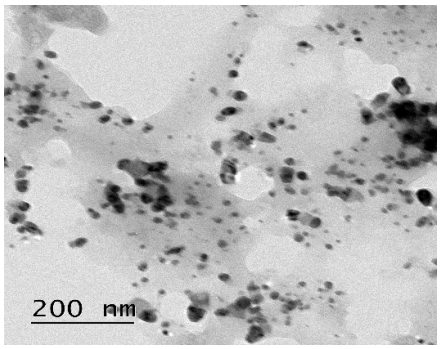

B1

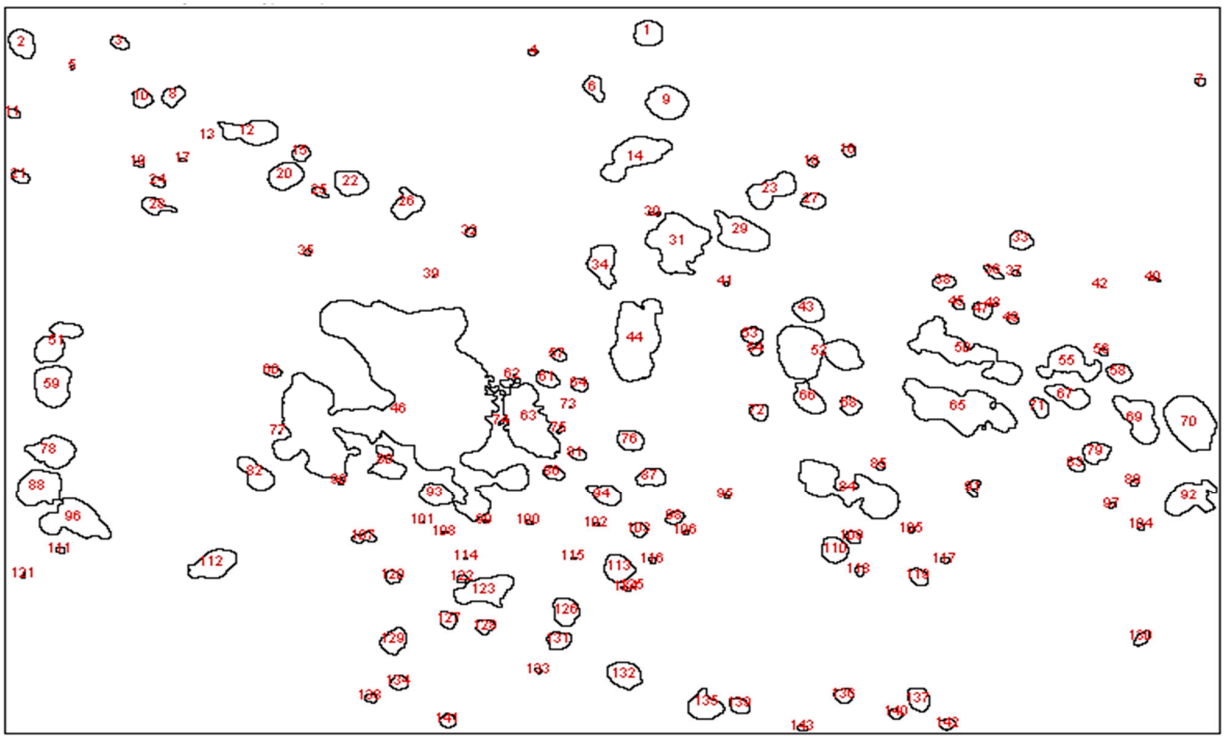

B2

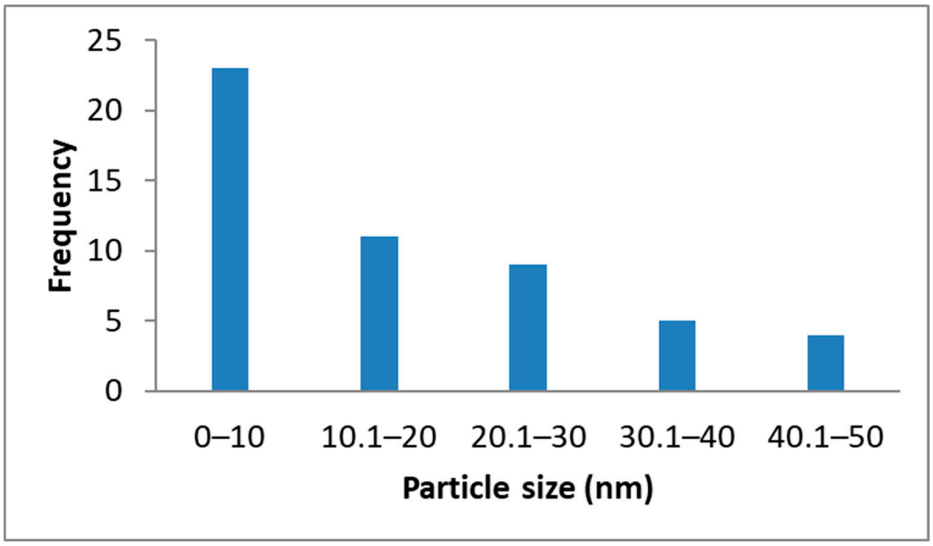

C

Figure 2. Morphological features of synthesized AgNPs. (**A**) SEM image at the 200 nm scale; (**B1**,**B2**) TEM images; (**C**) average size distribution histogram representing AgNP size range.

Table 1. Silver nanoparticle size distribution based on TEM data (Figure 2B2).

AgNP S. No.	Area (nm)	Radius (nm)	Diameter (nm)	AgNP S. No.	Area (nm)	Radius (nm)	Diameter (nm)	AgNP S. No.	Area (nm)	Radius (nm)	Diameter (nm)
1	306.77	9.881701	19.7634	49	42.923	3.696326	7.392652	97	16.412	2.28563	4.571261
2	304.245	9.840949	19.6819	50	1352.059	20.74546	41.49092	98	93.42	5.453122	10.90624
3	93.42	5.453122	10.90624	51	528.957	12.97584	25.95168	99	6.312	1.417453	2.834906
4	23.986	2.763148	5.526296	52	1512.388	21.94102	43.88204	100	12.624	2.004582	4.009163
5	6.312	1.417453	2.834906	53	146.442	6.827443	13.65489	101	1.262	0.633804	1.267608
6	178.002	7.527273	15.05455	54	53.022	4.108216	8.216433	102	7.575	1.552804	3.105607
7	32.823	3.23232	6.464641	55	646.363	14.34378	28.68755	103	93.42	5.453122	10.90624
8	165.378	7.255446	14.51089	56	26.511	2.904948	5.809895	104	21.461	2.613667	5.227334
9	554.205	13.28191	26.56382	57	64.384	4.527039	9.054078	105	15.149	2.195924	4.391847
10	142.654	6.738562	13.47712	58	186.839	7.711858	15.42372	106	10.099	1.792935	3.585869
11	46.71	3.855939	7.711878	59	643.838	14.31573	28.63146	107	90.895	5.378922	10.75784
12	541.581	13.12977	26.25953	60	70.696	4.74376	9.487519	108	5.05	1.267859	2.535718
13	1.262	0.633804	1.267608	61	145.179	6.797937	13.59587	109	75.746	4.910267	9.820534
14	866.025	16.60315	33.2063	62	2.525	0.896512	1.793023	110	278.996	9.42376	18.84752
15	113.618	6.013798	12.0276	63	1426.543	21.30923	42.61845	111	22.724	2.689476	5.378952
16	59.334	4.345873	8.691747	64	89.632	5.341421	10.68284	112	511.283	12.75722	25.51443
17	8.837	1.677172	3.354345	65	1804.008	23.96318	47.92636	113	328.231	10.22151	20.44302
18	35.348	3.354345	6.708689	66	338.33	10.37757	20.75513	114	2.525	0.896512	1.793023
19	26.511	2.904948	5.809895	67	345.905	10.4931	20.98619	115	3.787	1.097926	2.195851
20	378.728	10.97966	21.95932	68	147.704	6.856798	13.7136	116	17.674	2.37188	4.74376
21	89.632	5.341421	10.68284	69	665.299	14.55237	29.10474	117	21.461	2.613667	5.227334
22	349.692	10.55038	21.10076	70	1090.737	18.63311	37.26621	118	36.61	3.413698	6.827396
23	540.319	13.11446	26.22892	71	140.129	6.678659	13.35732	119	130.03	6.433496	12.86699
24	56.809	4.252397	8.504794	72	126.243	6.339119	12.67824	120	79.533	5.031517	10.06303
25	53.022	4.108216	8.216433	73	1.262	0.633804	1.267608	121	7.575	1.552804	3.105607
26	323.181	10.14257	20.28515	74	10.099	1.792935	3.585869	122	32.823	3.23232	6.464641
27	154.016	7.001775	14.00355	75	16.412	2.28563	4.571261	123	641.313	14.28763	28.57526
28	175.477	7.473695	14.94739	76	224.712	8.457429	16.91486	124	15.149	2.195924	4.391847
29	735.995	15.30603	30.61207	77	1.262	0.633804	1.267608	125	1.262	0.633804	1.267608
30	15.149	2.195924	4.391847	78	563.042	13.38738	26.77476	126	300.458	9.779511	19.55902
31	1285.151	20.22564	40.45128	79	231.024	8.575388	17.15078	127	117.406	6.113225	12.22645
32	39.135	3.529457	7.058914	80	345.905	10.4931	20.98619	128	107.306	5.844364	11.68873
33	175.477	7.473695	14.94739	81	73.221	4.827731	9.655462	129	255.01	9.009566	18.01913
34	443.112	11.87632	23.75265	82	377.466	10.96135	21.92271	130	77.008	4.951003	9.902006
35	16.412	2.28563	4.571261	83	88.37	5.303684	10.60737	131	178.002	7.527273	15.05455
36	71.958	4.785913	9.571826	84	1455.578	21.52499	43.04998	132	367.366	10.81371	21.62742
37	18.936	2.455101	4.910202	85	26.511	2.904948	5.809895	133	13.887	2.102468	4.204937
38	130.03	6.433496	12.86699	86	112.356	5.980306	11.96061	134	103.519	5.740309	11.48062
39	1.262	0.633804	1.267608	87	215.875	8.289463	16.57893	135	371.154	10.86932	21.73864
40	16.412	2.28563	4.571261	88	679.186	14.70346	29.40692	136	111.094	5.946625	11.89325
41	7.575	1.552804	3.105607	89	23.986	2.763148	5.526296	137	213.35	8.240842	16.48168
42	1.262	0.633804	1.267608	90	10.099	1.792935	3.585869	138	45.447	3.803451	7.606903
43	304.245	9.840949	19.6819	91	78.27	4.991406	9.982812	139	127.505	6.370725	12.74145
44	1542.686	22.15971	44.31941	92	636.263	14.23127	28.46253	140	51.76	4.059031	8.118062
45	45.447	3.803451	7.606903	93	300.458	9.779511	19.55902	141	88.37	5.303684	10.60737
46	1952.661	24.93094	49.86188	94	257.535	9.05406	18.10812	142	70.696	4.74376	9.487519
47	128.768	6.4022	12.8044	95	8.837	1.677172	3.354345	143	23.986	2.763148	5.526296
48	6.312	1.417453	2.834906	96	919.047	17.10386	34.20772				

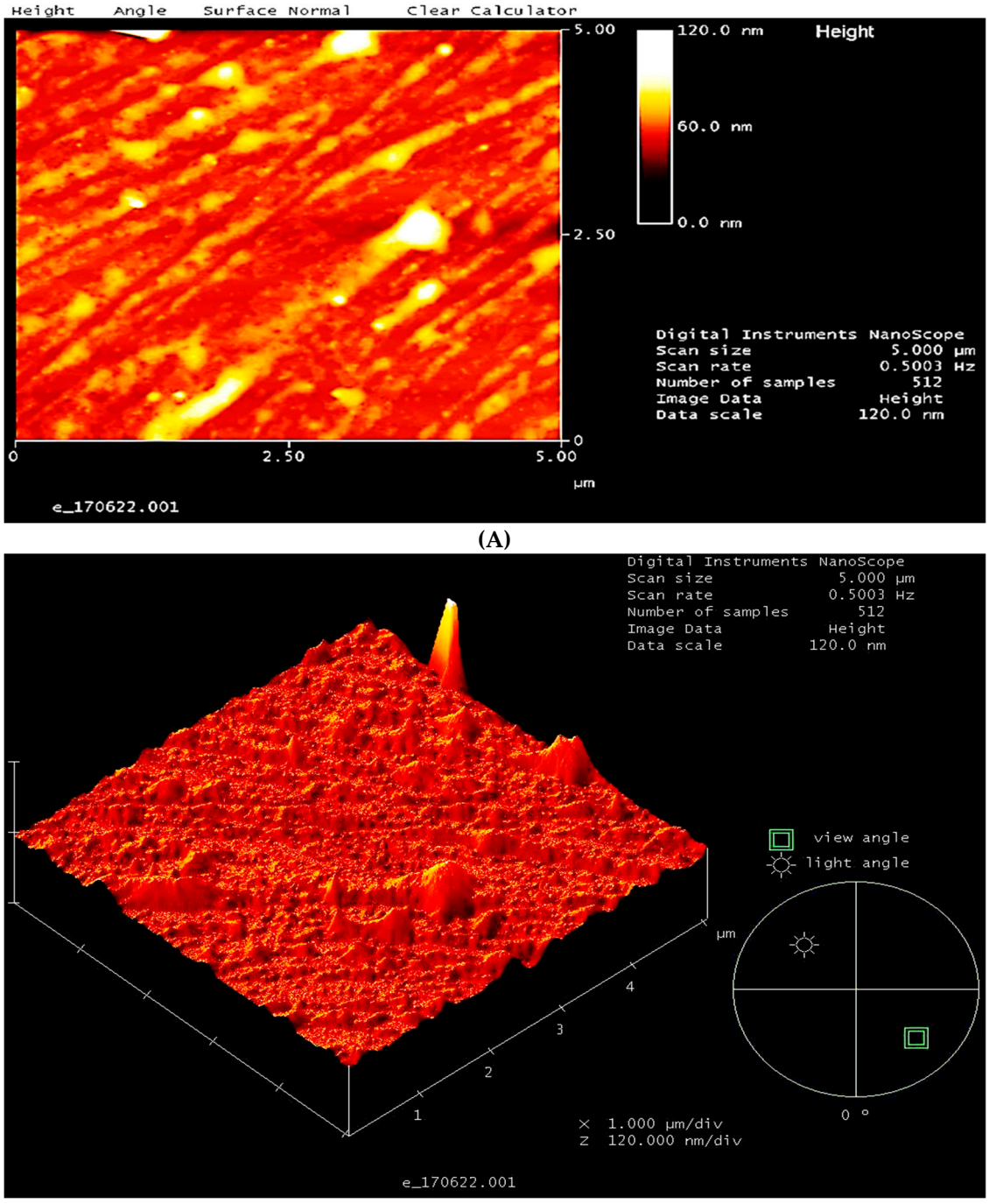

Figure 3. AFM images of AgNPs. (**A**) 2D image; (**B**) 3D image.

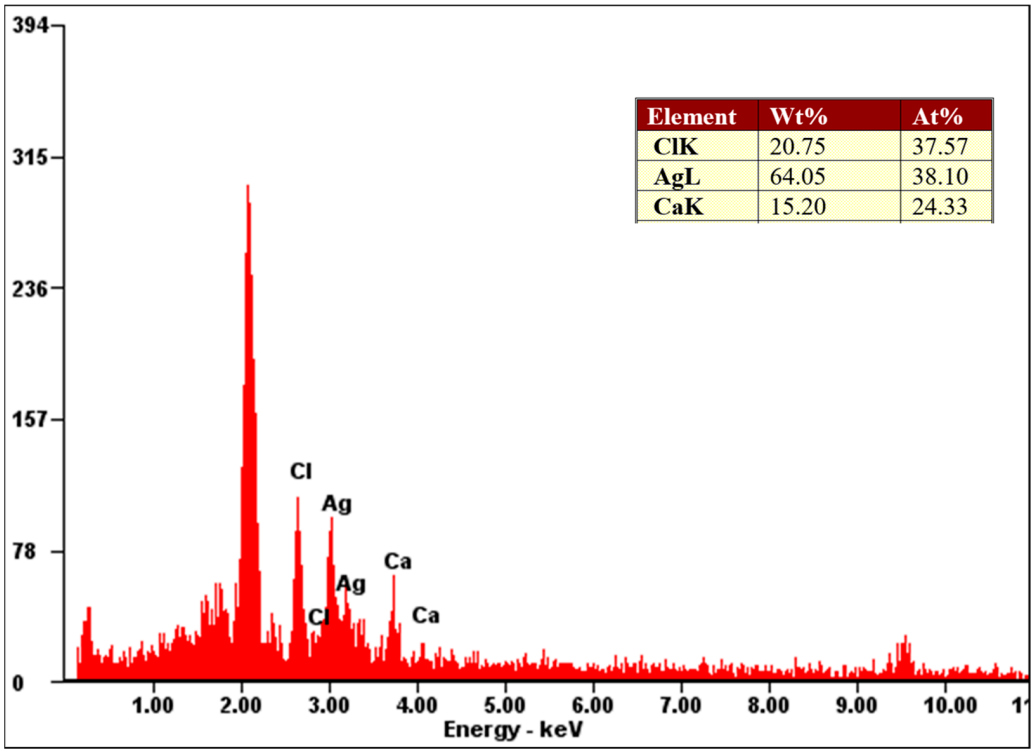

Figure 4. EDX spectrum of synthesized AgNPs.

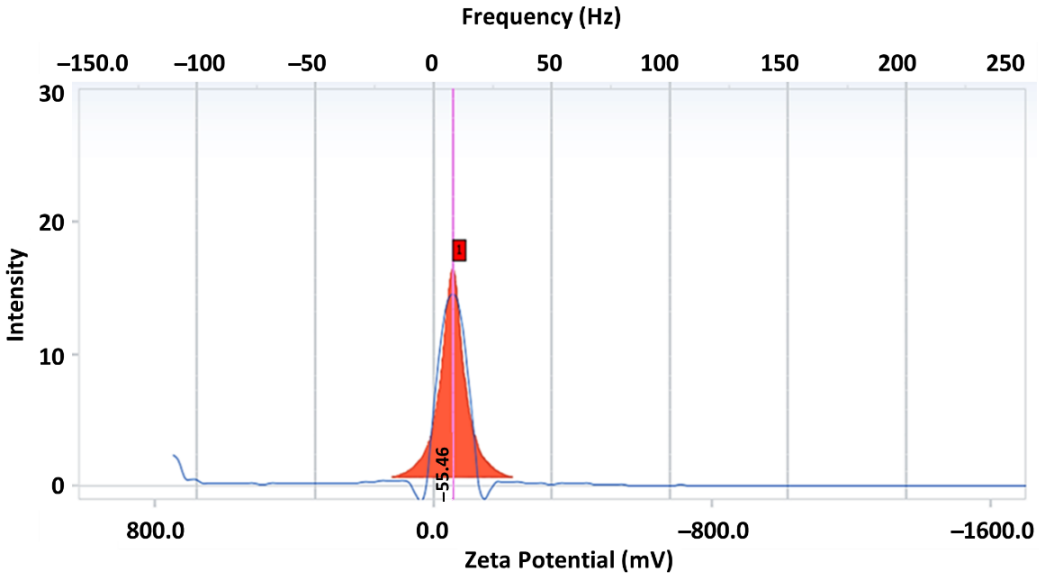

Figure 5. Zeta potential of synthesized AgNP from leaf extract of *C. indica.*

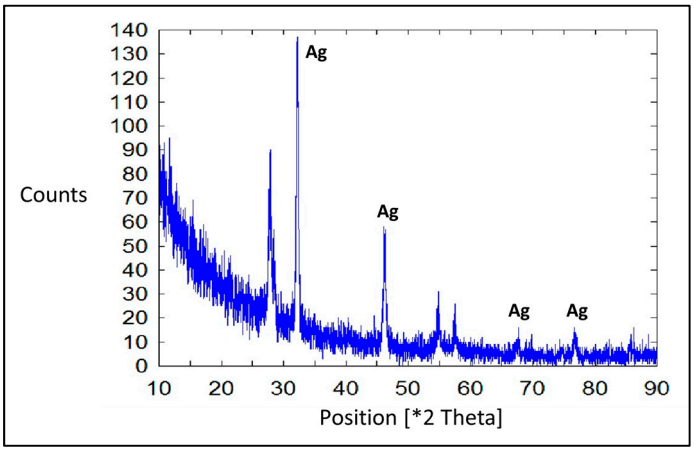

Figure 6. XRD spectrum of synthesized AgNPs.

3.2. Antibacterial Potential

The antimicrobial potential of CIL extract and AgNPs was evaluated against six Gram-positive bacteria *(S. haemolyticus*, *S. epidermidis*, *B. subtilis*, *Lactobacillus*, *S. aureus*, and *S. pyogenes)* and eight Gram-negative bacteria (*E. coli*, *P. mirabilis*, *S. typhi*, *E. cloacae*, *V. cholerae*, *P. aeruginosa*, *A. baumannii*, and *K. pneumoniae)*. Tables 2 and 3 present the zones of inhibition (ZOI) exhibited by AgNP and CIL extracts against each bacterial strain.

Table 2. Antibacterial activity of CIL ethanolic extract and synthesized AgNPs against Gram-positive bacteria.

Gram-Positive Bacteria	ZOI (mm)			
	CIL Extract (Ethanolic)	AgNP	Controls	
			Positive	Negative
S. haemolyticus	9	10.67 ± 0.33	25	NA
S. epidermidis	10.67 ± 0.67	11.67 ± 0.33	27 ± 1.00	NA
B. subtilis	9.33 ± 0.67	12.67 ± 1.20	25	NA
S. aureus	9.33 ± 0.33	11.67 ± 0.67	25.67 ± 0.67	NA
S. pyogenes	8.67 ± 0.33	9.67 ± 0.33	23.33 ± 0.33	NA
Lactobacillus	NA	11.67 ± 0.67	24.67 ± 0.67	NA

Note: The data are presented in the form of mean (±standard error), $p < 0.05$.

Table 3. Antibacterial activity of CIL ethanolic extract and synthesized AgNPs against Gram-negative bacteria.

Gram-Negative Bacteria	ZOI (mm)			
	CIL Extract (Ethanolic)	AgNP	Controls	
			Positive	Negative
P. mirabilis	NA	9.67 ± 0.33	25.33 ± 0.33	NA
S. typhi	9.33 ± 0.33	11.67 ± 0.33	30 ± 1.53	NA
V. cholerae	10.33 ± 0.33	12.67 ± 0.33	29.33 ± 0.67	NA
E. cloacae	10 ± 0.58	12	29.33 ± 0.67	NA
K. pneumoniae	9.33 ± 0.67	12 ± 0.58	26 ± 1.00	NA
E. coli	9.67 ± 0.33	10.33 ± 0.33	27 ± 1.00	NA
P. aeruginosa	10	11.33 ± 0.33	29.67 ± 0.33	NA
A. baumannii	NA	11.67 ± 0.88	NA	NA

Note: The data are presented in the form of mean (±standard error), $p < 0.05$.

The ZOI was calculated by measuring the zone in millimeters (mm). A clear ZOI indicates the inability of bacteria to grow or multiply around the sample-loaded disk

(Tables 2 and 3). The CIL extract inhibited growth of all test microorganisms except *Lactobacillus*, *P. mirabilis*, and *A. baumannii*. *Lactobacillus* is a non-pathogenic microorganism in which it produces lactic acid as a by-product of glucose metabolism. The bacterial species of the *Lactobacillus* genus (component of normal flora) are found in the gastrointestinal and genital tract of humans and animals [28]. Therefore, it is beneficial for humans that *Coccinia indica* plant extract did not exhibit any antimicrobial potential against *Lactobacillus*. The antimicrobial study of CIL extract against Gram-positive bacteria (GPB) revealed that CIL extract exhibited the maximum ZOI against *S. epidermidis* and the lowest ZOI against *S. pyogenes*, whereas the antimicrobial study of CIL extract against Gram-negative bacteria (GNB) revealed that CIL extract exhibited maximum ZOI against *V. cholerae* and a minimum ZOI against *S. typhi* and *K. pneumoniae*.

The antimicrobial activity of CIL extract was compared with the positive control (ciprofloxacin) and negative control (10% DMSO). The ZOIs of ciprofloxacin were larger and more clearly seen in comparison to those created by the CIL extract. *A. baumannii* did not show any ZOI in the ciprofloxacin disk. The resistance mechanism of *A. baumannii* is attributed to a single mutation that occurs from serine 83 to leucine in the quinolone resistance determining region (QRDRs) in gyrase subunit A (gyrA) [29].

The *C. indica* capped AgNPs exhibited substantial antimicrobial activity and ZOI against GPB and GNB. The AgNPs, when tested against GPB, exhibited the largest ZOI against *B. subtilis*, whereas when tested against GNB, they showed the largest ZOI against *V. cholerae*. The antimicrobial results revealed that the ZOI formed by AgNPs was larger than that formed by CIL extract. Large surface area per volume and easy penetrating characteristics of AgNPs best explain the antimicrobial activity of AgNPs. Therefore, AgNPs can easily diffuse through the cell walls of bacteria and disrupt microbial cell functions. The CIL extract comprises numerous components and has lesser penetration in comparison to AgNPs, which makes CIL extract less effective in damages bacterial cell walls [5]. Overall, in the present investigation, CIL extract and AgNPs displayed significant antimicrobial potential against GNB and GPB. The findings of present study are supported by previous studies that also reported the antimicrobial potential of *C. grandis* against *K. pneumonia*, *S. aureus*, and *B. cereus* [17].

4. Conclusions

The current research investigation shows that green synthesis of AgNP using an ethanolic extract of *C. indica* leaves is an eco-friendly, fast, and cost-effective method. In the present study, the antimicrobial activity of a 20 mg/mL concentration of CIL extract was shown to be sufficient to inhibit the growth of pathogenic bacteria. This study proves that compared to CIL extract, the ZOI of AgNP is larger against both GPB and GNB. Hence, the present study establishes the broad-spectrum antimicrobial potential of CIL extract derived AgNPs against Gram-negative and Gram-positive bacteria and recommends CIL ethanolic extract as an efficient biomaterial for green synthesis of silver nanoparticles.

Author Contributions: Conceptualization, S.V.C., S.S. (Sumitha Samuggam), S.C.B.G., G.R., P.A., L.V.R., N.K.F., and S.F.; validation, S.V.C., S.C.B.G., G.R., P.A., L.V.R., P.M., N.K.F., and S.F.; formal analysis, S.V.C., S.C.B.G., S.S. (Sumitha Samuggam), G.R., P.A., N.K.F., and S.F.; methodology, S.V.C., S.C.B.G., S.S. (Sumitha Samuggam), P.A., P.M., and K.K.; investigation, S.V.C., S.C.B.G., P.A., G.R., and L.V.R.; resources, S.V.C., S.C.B.G., P.A., L.V.R., N.K.F., S.F., G.R., and S.S. (Subramaniam Sreeramanan); data curation, S.V.C., S.C.B.G., P.A., L.V.R., N.K.F., S.F., G.R., and S.S. (Subramaniam Sreeramanan); writing—original draft preparation, S.V.C., S.C.B.G., P.A., L.V.R., N.K.F., S.F., G.R., and S.S. (Sumitha Samuggam); writing—review and editing, S.V.C., S.C.B.G., G.R., P.A., L.V.R., N.K.F., and S.F.; visualization, S.V.C., S.C.B.G., G.R., and P.A.; supervision, S.V.C.; project administration, S.V.C., S.C.B.G., and P.A.; funding acquisition, S.V.C. All authors have read and agreed to the published version of the manuscript.

Funding: This research was funded by the Ministry of Higher Learning Malaysia under the Fundamental Research Grant Scheme, FRGS/1/2018/STG03/AIMST/02/1. S.C.B.G. was supported by a special grant (9001-00596) from Universiti Malaysia Perlis.

Institutional Review Board Statement: Not applicable.

Informed Consent Statement: Not applicable.

Data Availability Statement: Not applicable.

Acknowledgments: The authors are thankful to Asian Institute of Medicine, Science and Technology AIMST University (Malaysia), Universiti Sains Malaysia (Malaysia), University Malaysia Perlis (Malaysia), Inha University (Korea), and Yogi Vemana University (India) for their support to successfully complete this study.

Conflicts of Interest: The authors have no conflict of interest to declare.

References

1. Sender, R.; Fuchs, S.; Milo, R. Revised estimates for the number of human and bacteria cells in the body. *PLoS Biol.* **2016**, *14*, e1002533. [CrossRef] [PubMed]
2. Hang, C.Z.; Fuloria, N.K.; Hong, O.J.; Kim, C.B.; Ting, B.Y.S.; Ru, C.S.; Ko, M.Y.; Fuloria, S. Biosynthesis of DLLAE blended silver nanoparticles and their response against periodontitis triggering bacteria. *Int. J. Res. Pharm. Sci.* **2020**, *11*, 1849–1856. [CrossRef]
3. Muthukumar, H.; Matheswaran, M. Amaranthus spinosus leaf extract mediated FeO nanoparticles: Physicochemical traits, photocatalytic and antioxidant activity. *ACS Sustain. Chem. Eng.* **2015**, *3*, 3149–3156. [CrossRef]
4. Song, J.Y.; Kim, B.S. Rapid biological synthesis of silver nanoparticles using plant leaf extracts. *Bioproc. Biosyst. Eng.* **2009**, *32*, 79. [CrossRef] [PubMed]
5. Ramanathan, S.; Gopinath, S.C.; Anbu, P.; Lakshmipriya, T.; Kasim, F.H.; Lee, C.-G. Eco-friendly synthesis of Solanum trilobatum extract-capped silver nanoparticles is compatible with good antimicrobial activities. *J. Mol. Struct.* **2018**, *1160*, 80–91. [CrossRef]
6. Fuloria, N.K.; Fuloria, S.; Chia, K.Y.; Karupiah, S.; Sathasivam, K. Response of green synthesized drug blended silver nanoparticles against periodontal disease triggering pathogenic microbiota. *J. Appl. Biol. Biotchnol.* **2019**, *7*, 46–56.
7. Gomathi, M.; Rajkumar, P.V.; Prakasam, A.; Ravichandran, K. Green synthesis of silver nanoparticles using Datura stramonium leaf extract and assessment of their antibacterial activity. *Res. Eff. Technol.* **2017**, *3*, 280–284. [CrossRef]
8. Mittal, J.; Jain, R.; Sharma, M.M. Phytofabrication of silver nanoparticles using aqueous leaf extract of *Xanthium strumerium* L. and their bactericidal efficacy. *Adv. Nat. Sci. Nanosci.* **2017**, *8*, 025011. [CrossRef]
9. Lade, B.D.; Shanware, A.S. Phytonanofabrication: Methodology and Factors Affecting Biosynthesis of Nanoparticles. In *Nanosystems*; Limited 5 Princes Gate Court; IntechOpen: London, UK, 2020. [CrossRef]
10. Makarov, V.V.; Makarova, S.S.; Love, A.J.; Sinitsyna, O.V.; Dudnik, A.O.; Yaminsky, I.V.; Taliansky, M.E.; Kalinina, N.O. Biosynthesis of stable iron oxide nanoparticles in aqueous extracts of Hordeum vulgare and Rumex acetosa plants. *Langmuir* **2014**, *30*, 5982–5988. [CrossRef]
11. El-Kassas, H.Y.; Aly-Eldeen, M.A.; Gharib, S.M. Green synthesis of iron oxide (Fe_3O_4) nanoparticles using two selected brown seaweeds: Characterization and application for lead bioremediation. *Acta Oceanol. Sin.* **2016**, *35*, 89–98. [CrossRef]
12. Silveira, C.; Shimabuku, Q.L.; Silva, M.F.; Bergamasco, R. Iron-oxide nanoparticles by the green synthesis method using Moringa oleifera leaf extract for fluoride removal. *Environ. Technol.* **2018**, *39*, 2926–2936. [CrossRef] [PubMed]
13. Dadgostar, P. Antimicrobial resistance: Implications and costs. *Infect. Drug Resist.* **2019**, *12*, 3903. [CrossRef] [PubMed]
14. Cheesman, M.J.; Ilanko, A.; Blonk, B.; Cock, I.E. Developing new antimicrobial therapies: Are synergistic combinations of plant extracts/compounds with conventional antibiotics the solution? *Pharmacogn. Rev.* **2017**, *11*, 57–72. [PubMed]
15. Hussein, R.A.; El-Anssary, A.A. Plants secondary metabolites: The key drivers of the pharmacological actions of medicinal plants. *Herb. Med.* **2018**. [CrossRef]
16. Shaheen, S.Z.; Bolla, K.; Vasu, K.; Charya, M.S. Antimicrobial activity of the fruit extracts of *Coccinia indica*. *Afr. J. Biotechnol.* **2009**, *8*, 7073–7076.
17. Sivaraj, A.; Jenifa, B.P.; Kavitha, M.; Inbasekar, P.; Senthilkumar, B.; Panneerselvam, A. Antibacterial activity of *Coccinia grandis* leaf extract on selective bacterial strains. *J. Appl. Pharm. Sci.* **2011**, *1*, 120–123.
18. Nitharwal, R.K.; Patel, H.; Karchuli, M.S.; Ugale, R.R. Chemoprotective Potential of Coccinia Indica against Cyclophos-phamide-Induced Toxicity. *Indian J. Pharmacol.* **2013**, *45*, 502.
19. Sumitha, S.; Vasanthi, S.; Shalini, S.; Chinni, S.V.; Gopinath, S.C.B.; Kathiresan, S.; Anbu, P.; Ravichandran, V. Durio zibethinus rind extract mediated green synthesis of silver nanoparticles: Characterization and biomedical applications. *Pharmacogn. Mag.* **2019**, *15*, 52.
20. Sumitha, S.; Vasanthi, S.; Shalini, S.; Chinni, S.V.; Gopinath, S.C.; Anbu, P.; Bahari, M.B.; Harish, R.; Kathiresan, S.; Ravichandran, V. Phyto-mediated photo catalysed green synthesis of silver nanoparticles using Durio zibethinus seed extract: Antimicrobial and cytotoxic activity and photocatalytic applications. *Molecules* **2018**, *23*, 3311. [CrossRef]
21. Anbu, P.; Gopinath, S.C.; Yun, H.S.; Lee, C.-G. Temperature-dependent green biosynthesis and characterization of silver nanoparticles using balloon flower plants and their antibacterial potential. *J. Mol. Struct.* **2019**, *1177*, 302–309. [CrossRef]
22. Buszewski, B.; Railean-Plugaru, V.; Pomastowski, P.; Rafińska, K.; Szultka-Mlynska, M.; Golinska, P.; Wypij, M.; Laskowski, D.; Dahm, H. Antimicrobial activity of biosilver nanoparticles produced by a novel Streptacidiphilus durhamensis strain. *J. Microbiol. Immunol. Infect.* **2018**, *51*, 45–54. [CrossRef] [PubMed]

23. Velusamy, P.; Su, C.-H.; Venkat Kumar, G.; Adhikary, S.; Pandian, K.; Gopinath, S.C.; Chen, Y.; Anbu, P. Biopolymers regulate silver nanoparticle under microwave irradiation for effective antibacterial and antibiofilm activities. *PLoS ONE* **2016**, *11*, e0157612. [CrossRef] [PubMed]
24. Aljabali, A.A.; Akkam, Y.; Al Zoubi, M.S.; Al-Batayneh, K.M.; Al-Trad, B.; Abo Alrob, O.; Alkilany, A.M.; Benamara, M.; Evans, D.J. Synthesis of Gold Nanoparticles Using Leaf Extract of Ziziphus Zizyphus and Their Antimicrobial Activity. *Nanomaterials* **2018**, *8*, 174. [CrossRef] [PubMed]
25. Saeb, A.; Alshammari, A.S.; Al-Brahim, H.; Al-Rubeaan, K.A. Production of Silver Nanoparticles with Strong and Stable Antimicrobial Activity against Highly Pathogenic and Multidrug Resistant Bacteria. *Sci. World J.* **2014**, *2014*, 704708. [CrossRef] [PubMed]
26. Suvith, V.S.; Philip, D. Catalytic degradation of methylene blue using biosynthesized gold and silver nanoparticles. *Spectrochim. Acta A Mol. Biomol. Spectrosc.* **2014**, *118*, 526–532. [CrossRef] [PubMed]
27. Fuloria, S.; Hong, O.; Kim, C.; Ting, B.; Karupiah, S.; Paliwal, N.; Kumari, U.; Sathasivam, K.; Vetriselvan, S.; Fuloria, N. Synthesis of Silver Nanoparticles of Corn Silk Agrowaste and Their Bioactivities. *Asian J. Chem.* **2020**, *32*, 1497–1504. [CrossRef]
28. Hynönen, U.; Palva, A. Lactobacillus surface layer proteins: Structure, function and applications. *Appl. Microbiol. Biotechnol.* **2013**, *97*, 5225–5243. [CrossRef]
29. Maleki, M.-H.; Jalilian, F.A.; Khayat, H.; Mohammadi, M.; Pourahmad, F.; Asadollahi, K.; Pakzad, I.; Sadeghifard, N.; Soroush, S.; Emaneini, M. Detection of highly ciprofloxacin resistance Acinetobacter baumannii isolated from patients with burn wound infections in presence and absence of efflux pump inhibitor. *Maedica* **2014**, *9*, 162.